Desalination and Water Treatment
www.deswater.com
doi: 10.1080/19443994.2015.1042060

57 (2016) 11326–11336
May

Taylor & Francis
Taylor & Francis Group

Potential efficacy of a mesoporous biosorbent *Simarouba glauca* seed shell powder for the removal of malachite green from aqueous solutions

B. Jeyagowri[a,*], R.T. Yamuna[b]

[a]*Department of Chemistry, Hindusthan College of Engineering and Technology, Coimbatore 641032, India, Tel. +91 989 424 5562; email: gowrivasuphd2010@gmail.com*
[b]*Department of Chemistry, Kalaignar Karunanidhi Institute of Technology, Coimbatore 641402, India, Tel. +91 984 256 3693; email: rtyamuna@gmail.com*

Received 9 August 2014; Accepted 9 April 2015

ABSTRACT

In this present study, formaldehyde-treated *Simarouba glauca* seed shell powder, a low-cost agricultural byproduct, was used as the adsorbent for the removal of cationic dye malachite green (MG) from aqueous solutions. The adsorbent was characterized by Fourier transform infrared spectroscopy, scanning electron microscopy, XRD, BET, and CHNS analyses. Batch mode adsorption studies were carried out under various experimental conditions such as agitation time, dye concentration, adsorbent dose, and pH to assess the potentiality of the adsorbent for the removal of MG from wastewater. Optimum adsorption of MG was found to be at pH 8 for an equilibrium time of 60 min with an adsorbent dose of 0.15 g. The experimental data were analyzed using Langmuir, Freundlich, Temkin, and Dubinin–Radushkevich isotherms. The data fitted well with Langmuir model with a maximum adsorption capacity of 125 mg/g. Kinetic data were analyzed using pseudo-first-order, pseudo-second-order, and intraparticle diffusion models. The experimental results showed that the pseudo-second-order model fits well.

Keywords: Biosorption; *Simarouba glauca* seed shell; Malachite green; Adsorption isotherm; Kinetic studies

1. Introduction

Dyes are widely used in various industries such as paper, textile, rubber, plastic etc., and the wastewater generated is of major environmental issue. The discharge of colored wastewater causes significant problems such as increasing toxicity, chemical oxygen demand, and reduction of the light penetration which has a derogatory effect on the photosynthetic phenomenon [1]. Thus, adequate treatment of wastewater containing dyes is of great importance for human health and environment.

Various conventional methods employed for the removal of dyes from aqueous solutions such as ion exchange, ultrafiltration, electrocoagulation, photo-oxidation, reverse osmosis, microwave oxidation etc., have significant disadvantages such as disposal of toxic sludge, high-energy requirement, and cost expensive [1,2]. Adsorption is one of the most efficient methods for the removal of dyes from wastewater, which implies the use of activated carbon as the adsorbent. The activated carbon is a very

*Corresponding author.

efficient adsorbent in the removal of dyes from aqueous solution due to its high surface area and porosity. However, due to high cost of activated carbon, its use in the field is restricted on economical consideration. The use of natural biomaterials is a promising alternative due to their relative abundance and low commercial value [3,4]. A number of low-cost biomaterials as adsorbents are reported in the literature. These include waste biogas residual slurry [5], asoka leaf [6], watermelon peel [7], garlic peel [1], hazelnut shell [8], neem saw dust [9], papaya seeds [10], pigeon peas hulls [11], jujuba seeds [12], pine cone [13], oil palm empty fruit bunch fibers [14], wood apple shell [15], water hyacinth [16], egg shells [17], and pine saw dust [18]. The direct application of these materials was found to be limited due to leaching of organic substances such as lignin, tannin, pectin, and cellulose from the solution. To overcome such problems, chemical treatment on solid adsorbents has been used as a technique for improving physical and chemical properties of them and to increase their adsorption capacity [19].

Malachite green (MG), a triarylmethane dye has been extensively used in aquaculture industries as parasiticide. It is also commonly used as a food coloring agent, food additive, medical disinfectant, and for dyeing of cotton, silk, leather, paper, jute, wool, etc. However, MG now generated a major environmental concern due to its effects on immune system and reproductive system as well as its genotoxic and carcinogenic potentials [17,18,20]. Therefore, removal of MG from effluents has now become very essential to protect our water resources.

Simarouba glauca, commonly known as paradise tree is an edible oil seed-bearing tree well suited for warm, humid, and tropical regions. This eco-friendly tree with well-developed root system and with evergreen dense canopy efficiently checks soil erosion, supports soil microbial life, and improves groundwater position. The seed contains about 50–60% oil with 63% unsaturated fatty acid among which 59.1% is oleic acid and is fit for human consumption. Many research studies are going on in efficient usage of biodiesel from *S. glauca* seed oil [21]. The seed shell, a waste product from this eco-friendly tree has been used for the present study for the removal of MG from aqueous solutions. The main objective of the present study is to investigate the feasibility of formaldehyde-treated *S. glauca* seed shell in the removal of MG from aqueous solutions. The effect of pH, initial dye concentration, adsorption isotherm, and kinetic parameters for the biosorption were evaluated.

2. Materials and methods

2.1. Materials

S. glauca seed shells were collected from Gujarat, India, and the dye MG was purchased from SFCL Limited, New Delhi.

2.2. Preparation of the adsorbent (SFTS)

The seed shells were powdered and were steam activated for 40 min and then washed well with distilled water. The washed material was then treated with 1% formaldehyde in the ratio 1:5 and was heated in a hot air oven at 50˚C for 4 h. The seed shell powder was filtered, washed again with distilled water to remove free formaldehyde, and activated at 80˚C in a hot air oven for 24 h. The treated material (SFTS) was sieved for the particle size 75–150 μm and stored in an airtight plastic container for further use.

2.3. Characterization of the adsorbent

The adsorbent was characterized using Fourier transform infrared spectroscopy (FTIR) spectra and scanning electron microscopy (SEM, JSM-6390, JOEL). The infrared spectra of the sample were obtained using a Fourier transform infrared spectrometer (Shimadzu, model IRAffinity-1). The surface area, pore volume, and average pore diameter were determined by nitrogen sorption at 77 K (Micromeritics, ASAP 2010). The X-ray diffractograms were obtained using PANalytical X'Pert PRO, PANalytical B.V., Almelo, The Netherlands. The surface morphological features of the sample were obtained using SEM. The elemental analysis of the sample was carried out using Elementar Vario EL III. The zero point of charge of the adsorbent was also determined.

2.4. Adsorption experiments

A stock solution of the dye MG (1,000 mg/L) was prepared by dissolving 1 g of the dye in 1 L of distilled water, which was diluted to a desired concentration. Batch adsorption experiments were carried out by adding 0.1 g of SFTS into 250-mL Erlenmeyer flasks containing 50 mL of different initial concentrations (60, 120, 300, and 400 mg/L) of MG solution. The flasks were agitated in a rotary shaker at room temperature until equilibrium was reached. The adsorbent was separated by filtration and the concentration of MG in the supernatant was determined at λ_{max} 617 nm by Visible spectrophotometer (Shimadzu Visible Spectrophotometer UVmini-1240 V).

The amount of dye adsorbed onto SFTS was calculated by the following equation:

$$q_e = [(C_0 - C_e) \times V]/M \quad (1)$$

where q_e is amount of dye adsorbed at time of equilibrium time (mg/g), C_0 and C_e are the initial and equilibrium dye concentrations (mg/L) in the solution. V is the volume (L) of the solution and M is the mass of the adsorbent (g).

To investigate the effect of pH on dye adsorption, 0.1 g of SFTS was agitated with 50 mL of MG solution of concentration 300 mg/L in a rotary shaker. The experiment was conducted by varying the pH from 2 to 11 using 0.1 M HCl and 0.1 M NaOH. The effect of adsorbent dose on the equilibrium uptake of 300 mg/L of MG was investigated using various adsorbent dosages between 0.05 and 0.2 g, respectively. All studies were carried out at equilibrium time of 60 min and at a temperature of 30 ± 2°C.

2.5. Desorption studies

Desorption studies were carried out using three desorbing solvents (H_2O, HCl, and CH_3COOH). After adsorption experiments, the MG-loaded SFTS was separated out by filtration using Whatman filter paper No. 42 and the filtrate was discarded. The MG-loaded SFTS was given a gentle wash with distilled water to remove the unadsorbed MG if present. The dye-loaded samples were agitated with distilled water, 0.1 M HCl, and 0.1 M CH_3COOH [22] for 60 min. The desorbed MG in the solution was separated and analyzed as before. The percentage of desorption was calculated.

3. Results and discussion

3.1. Physical characterization of the adsorbent

3.1.1. Structural characterization studies

The FTIR spectrum of SFTS before and after adsorption was shown in Fig. 1. Wide band around 3,356 cm^{-1} was due to stretching vibration of O–H bond in hydroxyl groups. The peaks observed at 2,935 and 1,334 cm^{-1} correspond to the C–H stretching and bending vibration of methyl groups, respectively. Absorption band at 1,722 cm^{-1} is characteristic to

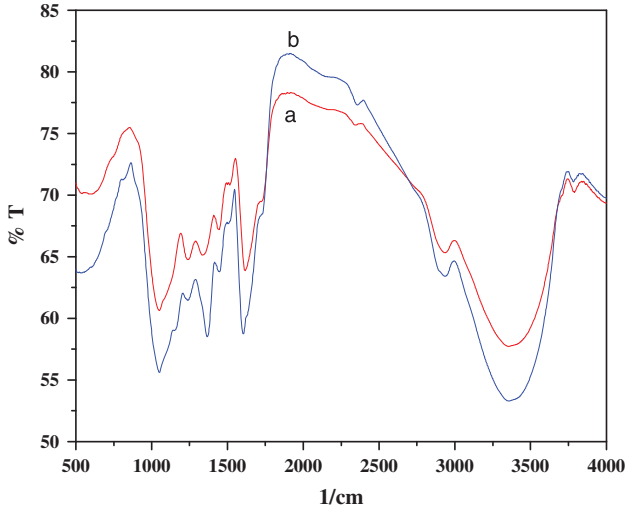

Fig. 1. FTIR spectrum of SFTS (a) before and (b) after adsorption.

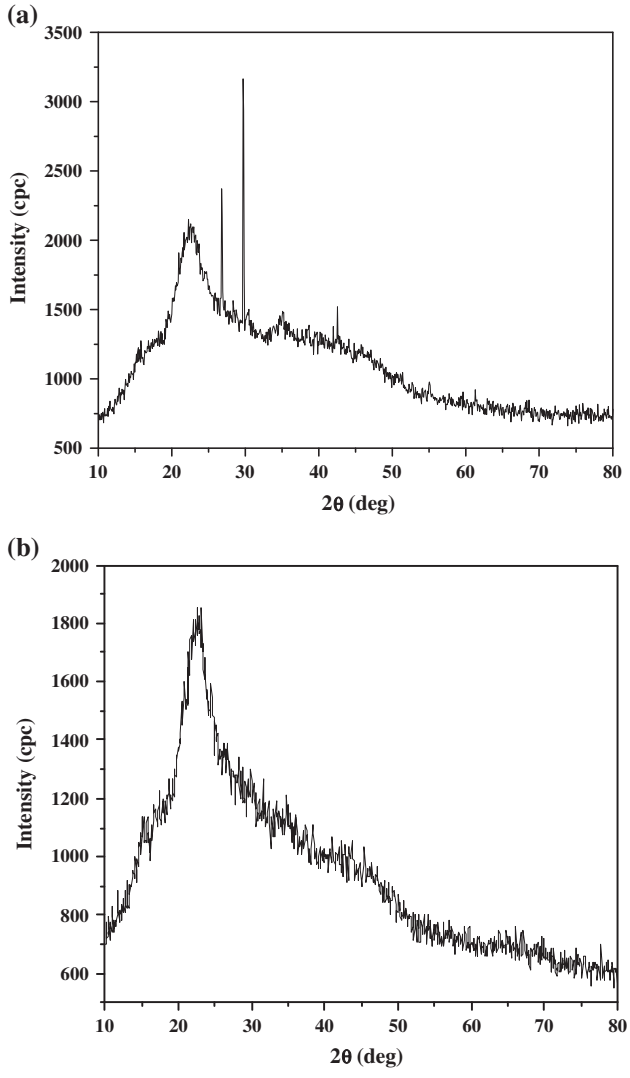

Fig. 2. X-ray diffraction pattern of SFTS (a) before adsorption and (b) after adsorption.

carbonyl group stretching. The absorption bands at 1,616 and 1,516 cm^{-1} were due to aromatic C=C stretching in phenyl ring of the lignin structure. Absorption band at 1,446 cm^{-1} may be attributed to the methoxy group of lignin in SFTS. The strong band at 1,049 cm^{-1} also confirms the lignin structure of SFTS. The absorption band at 1,240 cm^{-1} may be due to the C–O stretching in phenols [23,24]. The disappearance of absorption band at 1,722 cm^{-1} in Fig. 1 after adsorption indicates the possibility of involvement of surface functional groups in the adsorption process. The XRD patterns of the adsorbent SFTS and dye-loaded SFTS were presented in Fig. 2. The XRD pattern of the SFTS has well-defined peaks which confirm the crystalline nature of the adsorbent. The XRD pattern of dye-loaded SFTS clearly indicates the amorphous nature of the adsorbent after adsorption and suggests the diffusion of dye molecules into the mesopores and adsorbed mostly by chemisorption which alters the structure of SFTS after adsorption [25]. The elemental analysis of SFTS was also done and the composition is shown in Table 1.

3.1.2. Surface morphological studies

The evaluation of the textural structure of adsorbent surface was done using the SEM microscopic images of SFTS before and after adsorption (Fig. 3). The SEM image of SFTS clearly shows the irregular, rough, and porous surface nature of the adsorbent and the SEM image of SFTS after adsorption clearly indicates the complete coverage of the adsorbent surface with dye molecules. The BET surface area, total pore volume, and average pore diameter of SFTS were given in Table 1. The pore size distribution of SFTS is shown in Fig. 4. It is seen from the figure that most pores of SFTS are in the mesoporous range (diameter 2–50 nm) [26]. The average pore diameter of SFTS (Table 1) confirms the mesoporous nature of SFTS.

Table 1
Physicochemical characterization of SFTS

Parameters	Values
BET surface area	1.8704 m^2/g
Total pore volume	0.003948 cm^3/g
Average pore diameter	8.4422 nm
Zero point of charge (pH_{zpc})	3.8
C %	52.21
H %	7.07
N %	1.32
S %	0.32

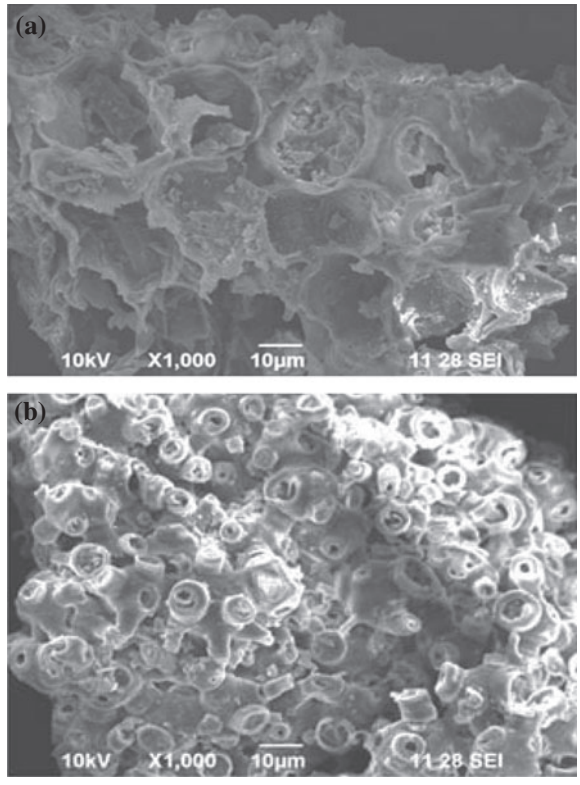

Fig. 3. SEM image of SFTS (a) before adsorption and (b) after adsorption.

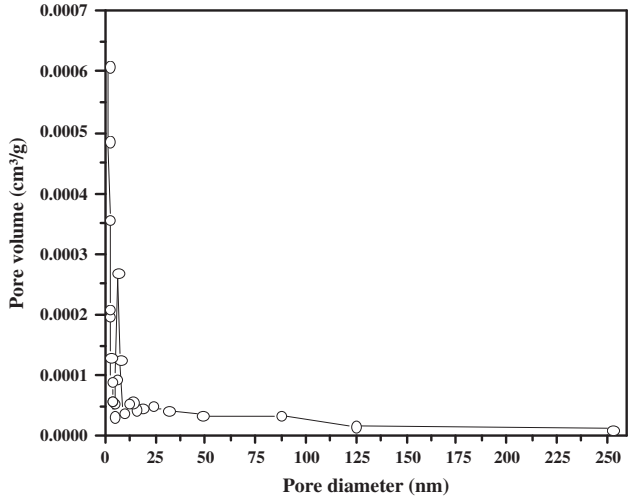

Fig. 4. Pore size distribution of SFTS.

3.2. Effect of initial dye concentration and contact time

The effect of initial dye concentration and contact time on the adsorption of MG is shown in Fig. 5. The removal of the dye MG by the SFTS increased with

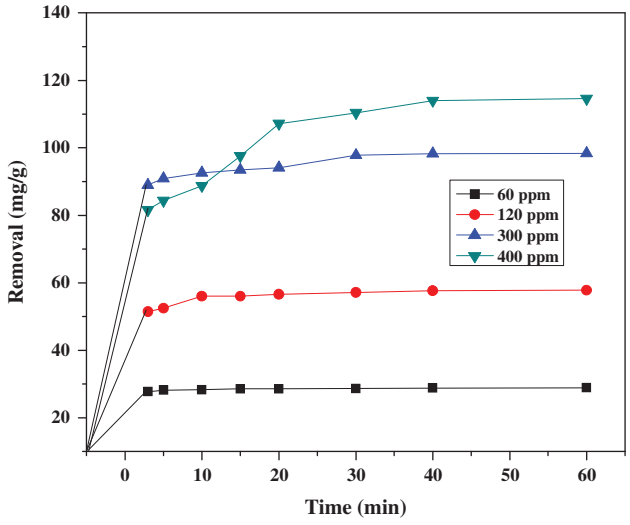

Fig. 5. Effect of contact time on the adsorption of MG onto SFTS (adsorbent dose = 0.1 g/50 mL).

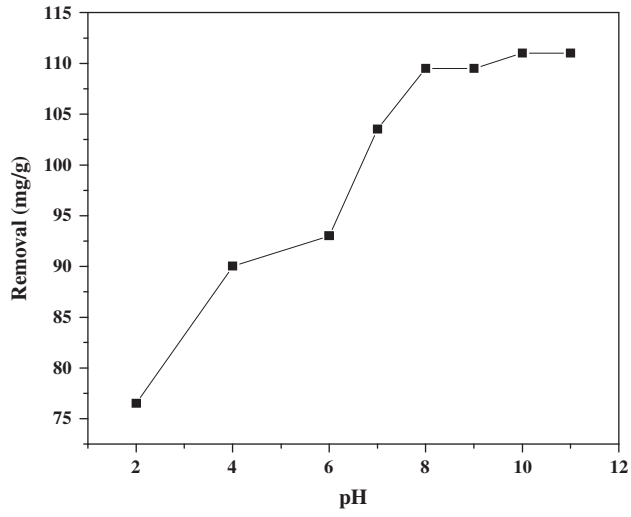

Fig. 6. Effect of pH on the adsorption of MG onto SFTS (adsorbent dose = 0.1 g/50 mL, C = 300 mg/L, and t = 60 min).

increase in time and attained equilibrium at 60 min. The removal of MG at equilibrium increased from 28.83 to 114 mg/g with increase in dye concentration from 60 to 400 mg/L. It is clear from the Fig. 5 that the extent of adsorption was found to increase with increase in initial dye concentration. The equilibrium time for the adsorption of MG onto SFTS at various adsorbate concentrations was found to be 60 min, which shows that the equilibrium concentration is independent of the initial adsorbate concentration. The plots are single, smooth, and continuous leading to saturation, suggesting the possibility of formation of monolayer coverage of the dye [27].

3.3. Effect of pH

The initial pH of the dye solution plays a significant role in the adsorption capacity of the adsorbent. The pH of the solution influences the surface properties of the adsorbent and ionization/dissociation of the adsorbate molecule. Fig. 6 shows the influence of pH on the removal capacity of SFTS. The adsorption of MG was found to be lower under acidic conditions and became higher as the pH increased. This could be explained on the basis of zero point of charge (pH_{zpc}) of SFTS which was determined to be at pH 3.8. The presence of excess H^+ ions at pH less than the pH_{zpc} compete with the dye cations causing less dye adsorption at acidic pH. However, at pH higher than pH_{zpc}, surface of SFTS becomes negatively charged and there exists a strong electrostatic attraction of dye cations with the adsorbent surface. This effect can be observed with increase in MG adsorption from 76.5 to 111 mg/g at pH 2–11 [28]. The optimum pH for the removal of MG was found to be at pH 8.0. Similar effect was observed in the adsorption of MG dye from aqueous solutions on sea shell powder [29] and activated carbon from rambutan peel [30].

3.4. Effect of adsorbent dosage

Fig. 7 shows the effect of adsorbent dose on the adsorption efficiency of the adsorbent SFTS. The adsorption increased from 44.9 to 83% as the adsorbent dose increased from 0.05 to 0.2 g per 50 mL of dye solution. Increase in adsorption with increase in adsorbent dose is due to the increase in surface area and availability of adsorption sites.

3.5. Isotherm analysis

Adsorption isotherm expresses the relation between the molecules distributed between liquid phase and solid phase in the equilibrium state. Adsorption isotherms help to understand the nature of interaction between adsorbate and adsorbent used for removal of organic pollutants in wastewater [31]. Adsorption isotherms are highly useful in evaluating the adsorption capacity of the adsorbent and thermodynamic parameters like energy of adsorption. The adsorption isotherm parameters provide significant information regarding adsorption mechanisms, surface properties, and affinities of the adsorbent [32].

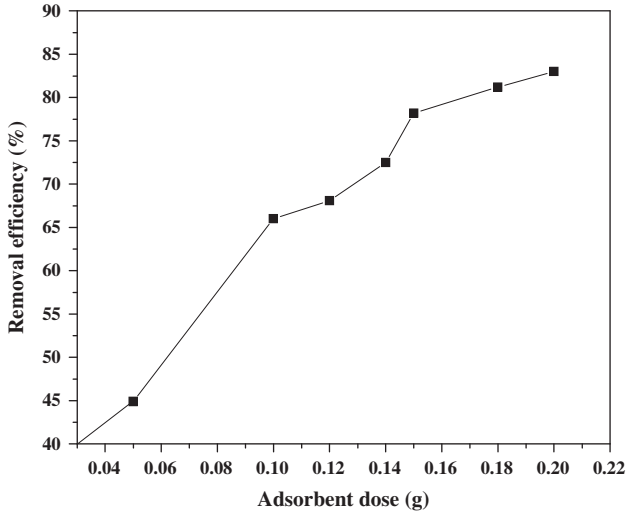

Fig. 7. Effect of adsorbent dose on adsorption of MG onto SFTS (V = 50 mL, initial concentration = 300 mg/L, pH 5.4, and t = 60 min).

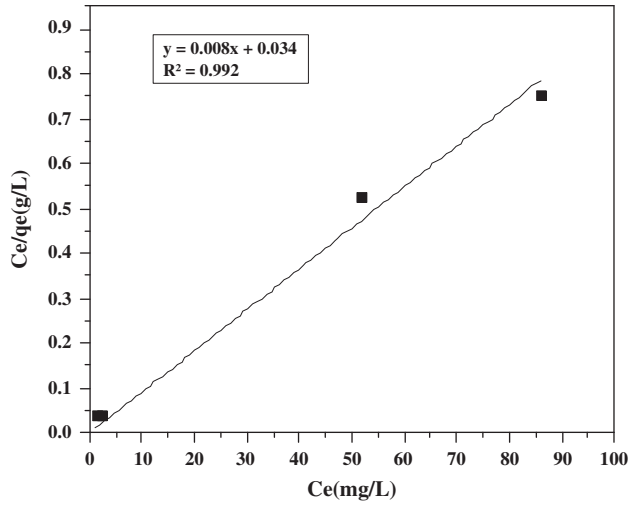

Fig. 8. Langmuir adsorption isotherm for the adsorption of MG onto SFTS.

The equilibrium isotherm equations were used to describe the experimental data. In this present study, Langmuir, Freundlich, Temkin, and Dubinin–Radushkevich isotherm models were used to fit the experimental data of adsorption equilibrium of SFTS–MG system.

3.5.1. Langmuir adsorption isotherm

The Langmuir isotherm treats surface sites analogous to dissolved equilibrium constant with a mass balance on the total number of adsorption sites. The isotherm is valid for monolayer adsorption onto a surface containing a finite number of identical sites. The model assumes uniform energies of adsorption onto the surface and no transmission of adsorbate in the plane of the surface. The Langmuir isotherm is represented by the following equation [33]:

$$C_e/q_e = 1/Q_0 b + C_e/Q_0 \quad (2)$$

where C_e (mg/L) is the equilibrium concentration of MG, q_e (mg/g) is the amount of MG adsorbed at equilibrium time, and Q_0 and b are Langmuir constants related to adsorption capacity and energy of adsorption, respectively. A linear plot of C_e/q_e vs. C_e shows that the adsorption follows Langmuir isotherm model (Fig. 8). Q_0 and b were determined from slope and intercept of the linear plot and are presented in Table 2.

The essential characteristics of Langmuir adsorption isotherm can be expressed in terms of a dimensionless constant separation factor or equilibrium parameter R_L defined by

$$R_L = 1/(1 + K_L C_0) \quad (3)$$

where C_0 is initial metal ion concentration (mg/L) and K_L is the Langmuir constant (L/mg). R_L values imply the adsorption to be unfavorable ($R_L \geq 1$), linear ($R_L = 1$), favorable ($0 < R_L < 1$), or irreversible ($R_L = 0$) [33]. R_L values between 0 and 1 indicate favorable adsorption of MG onto SFTS. The comparison of adsorption capacities (Q_0) of various adsorbents is presented in Table 3.

Table 2
Isotherm parameters for the adsorption of MG onto SFTS

Isotherm	Parameters	Values
Langmuir	Q_0 (mg/g)	125
	b (L/mg^{-1})	0.235
	R^2	0.999
Freundlich	K_f (L/g)	34.81
	n	3.703
	R^2	0.885
Temkin	K_T (L/g)	6.8
	b (kJ/mol)	17.51
	R^2	0.961
D–R	Q_m (mol/g)	100.23
	E (kJ/mol)	1.0
	R^2	0.970

Table 3
Comparison of adsorption capacities of various low-cost adsorbents for MG

Adsorbents	Q_0 (mg/g)	Refs.
Simarouba glauca seed shell powder	125	This study
Oil palm trunk fiber	149.35	[34]
Asoka leaf powder	83.3	[6]
Neem saw dust	4.23	[9]
Rattan saw dust	62.7 ± 1.27	[3]
Hen feathers	2.82(10^{-5} mol/g)	[35]
Potato plant wastes		
Potato plant stem powder	27.0	[36]
Potato leaves powder	33.3	[36]
Treated ginger waste	84.03	[37]
Bivalve shell-*z. mays* L.		
Husk leaf	81.5	[38]
Native rice straw	94.34	[28]
Citric acid-modified rice straw	256.41	[28]
Sea shell powder	42.331	[29]

3.5.2. Freundlich isotherm

The Freundlich isotherm assumes a heterogeneous adsorption surface and active sites with different energies. The Freundlich isotherm is expressed as [39]:

$$q_e = K_f\, C_e^{1/n} \tag{4}$$

where K_f and n are Freundlich constants, where K_f (L/g) is the adsorption capacity of the sorbent and n (g/L) indicates the favorability of the adsorption process. Values of $n > 1$ represent the favorable adsorption condition. The linear form of the equation is expressed as

$$\ln q_e = \ln K_f + 1/n \ln C_e \tag{5}$$

The values of K_f and n were calculated from the intercept and slope of linear plot of ln q_e vs. ln C_e. The Freundlich isotherm parameters are presented in Table 2. Values of $n > 1$ represent the favorable adsorption of MG onto SFTS.

3.5.3. Temkin isotherm

Temkin isotherm assumes that along with saturation of adsorption sites during adsorption, the energy of adsorption decreases linearly rather than exponentially as implied by the Freundlich isotherm. The Temkin isotherm is expressed as [40]:

$$q_e = B_T \ln K_T\, C_e \tag{6}$$

where $B_T = RT/b$, R is the universal gas constant (8.314 J/mol/K), T is the absolute temperature (K), b is a Temkin constant related to adsorption energy (kJ/mol), and K_T is the binding energy (L/g). The linear form of this isotherm is given as

$$q_e = B_T \ln K_T + B_T \ln C_e \tag{7}$$

A plot of q_e vs. ln C_e enables the determination of constants K_T and b. The values of parameters are presented in Table 2.

3.5.4. Dubinin–Radushkevich (D–R) isotherm

D–R isotherm is applied to estimate the characteristic porosity and apparent free energy of adsorption. D–R isotherm is a more general approach compared to the Langmuir adsorption isotherm, as it does not assume homogeneous nature of the adsorbent surface or constant adsorption potential. The D–R isotherm determines the nature of the biosorption process. The linear form of this isotherm can be written as [41]:

$$\ln Q_e = \ln Q_m - \beta\varepsilon^2 \tag{8}$$

where Q_e is the amount of adsorbate adsorbed per g of adsorbent (mol/g), Q_m represents the maximum adsorption capacity of sorbent (mol/g), and β is a constant related to sorption energy (mol^2/J^2). ε, the Polanyi potential represents the work required to remove a molecule from its location, can be calculated as follows:

$$\varepsilon = RT\ln\left(1 + 1/C_e\right) \quad (9)$$

where R is the universal gas constant (kJ/mol-K), T is the absolute temperature (K), and C_e (mol/L) is the equilibrium concentration of adsorbate in solution. β is related to the mean free energy of sorption per mole (E, J/mol) of sorbate transferred from infinity in the solution to the adsorbent surface. The values of β and Q_m can be obtained from the plot of ln Q_e vs. ε^2. The mean free energy (E) can be calculated using the following relation

$$E = (-2\beta)^{1/2} \quad (10)$$

The mean free energy (E) of adsorption determines the nature of adsorption as physisorption or chemisorption. Physisorption occurs if the value of $E < 8$ kJ/mole, while $8 < E < 16$ kJ/mol describes chemisorption. The D–R isotherm parameters are presented in Table 2. The maximum adsorption capacity Q_m obtained using D–R isotherm for adsorption of MG onto SFTS is 100.23 mol/g. The value of E calculated is 1 kJ/mol and indicates the physical adsorption of MG onto SFTS [42,43].

The experimental data fitted to all four isotherms revealed that among all four isotherms, experimental data fits well to the Langmuir adsorption isotherm with $R^2 = 0.999$ and q_e^{cal} correlates with the observed values compared to the other three isotherms. The applicability of the Langmuir adsorption isotherm to MG adsorption shows that monolayer adsorption on the surface of the adsorbent is possible.

3.6. Kinetic studies

The kinetic studies of the adsorption process provide significant information about the mechanism of adsorption process. The three common models used to describe adsorption behavior are Lagergren's pseudo-first-order, Ho's pseudo-second-order, and Weber–Morris's intraparticle diffusion models.

The adsorption kinetics of MG onto SFTS was investigated with the help of these models and experimental data were analyzed.

3.6.1. Pseudo-first-order kinetic model

The pseudo-first-order model was based on the assumption that adsorption rate is proportional to the number of free sites available.

A linear form of the pseudo-first-order model was represented in the form [44]:

$$\log\left(q_e - q_t\right) = \log q_e - (K_1 t)/2.303 \quad (11)$$

where q_e and q_t are the amounts of dye adsorbed at equilibrium and at time t (mg/g), respectively, and K_1 (min^{-1}) is the rate constant of adsorption. The values of K_1 and q_e^{cal} were calculated from the slope and intercept of the plot of log (q_e–q_t) vs. t and represented in Table 4. The correlation coefficient is low and q_e^{cal} value did not show good agreement with the experimental one. This suggests that adsorption kinetics of MG onto SFTS does not follow the first-order kinetics.

3.6.2. Pseudo-second-order kinetic model

This model is based on the assumption that adsorption follows second-order chemisorption. The linear form of the pseudo-second-order model was represented as [44]:

$$t/q_t = 1/K_2 q_e^2 + t/q_e \quad (12)$$

where K_2 is the rate constant of adsorption (g/mg min), q_e and q_t are amounts of dye adsorbed (mg/g) at equilibrium and time t, respectively (min).

Table 4
Kinetic parameters for the adsorption of MG onto SFTS

Conc MG		Pseudo-first-order			Pseudo-second-order			Intraparticle diffusion	
(mg/L)	q_e^{exp} (mg/g)	q_e^{cal} (mg/g)	K_1 (min^{-1})	R^2	q_e^{cal} (mg/g)	K_2 (g/mg min)	R^2	K_{id}	R^2 (mg/g $min^{1/2}$)
60	28.83	1.079	0.033	0.936	29.41	0.2312	1	0.205	0.858
120	57.7	6.714	0.039	0.93	58.82	0.036	1	1.314	0.834
300	98.3	14.92	0.041	0.843	100	0.167	0.999	1.993	0.97
400	114	48.3	0.037	0.957	125	0.008	0.996	7.696	0.958

The values of K_2 and q_e^{cal} were calculated from the intercept ($1/K_2\ q_e^2$) and slope ($1/q_e$) of the plot t/q_t vs. t in Fig. 9, respectively, and presented in Table 4. It can be seen from Table 4 that q_e^{exp} was found to be in good agreement with q_e^{cal} values for the pseudo-second-order model. The higher correlation coefficient also suggests the applicability of the pseudo-second-order model for adsorption of MG onto SFTS.

3.6.3. Intraparticle diffusion model

The process of adsorption is a multistep process which involves three basic types: (1) transportation of the adsorbate from aqueous solution onto the surface of the solid adsorbent, (2) diffusion of the adsorbate into the pores of the adsorbent, a slow process and rate determining (intraparticle diffusion), and (3) binding of adsorbate molecules to the active sites in the pores of the adsorbent. The binding of adsorbate molecules to the active sites is the fastest stage. It is assumed that this stage does not limit mass transfer. The surface diffusion may slow down the kinetics of adsorption process [45]. Generally, in batch adsorption studies, intraparticle diffusion is often the rate-limiting step [44]. Weber intraparticle diffusion model is used to investigate the mechanism and rate-controlling steps affecting the adsorption kinetics. The experimental results were fitted to Weber intraparticle diffusion model and analyzed to elucidate diffusion mechanism. Intraparticle diffusion model is expressed as

$$q_t = K_{id} t^{1/2} + C_i \quad (13)$$

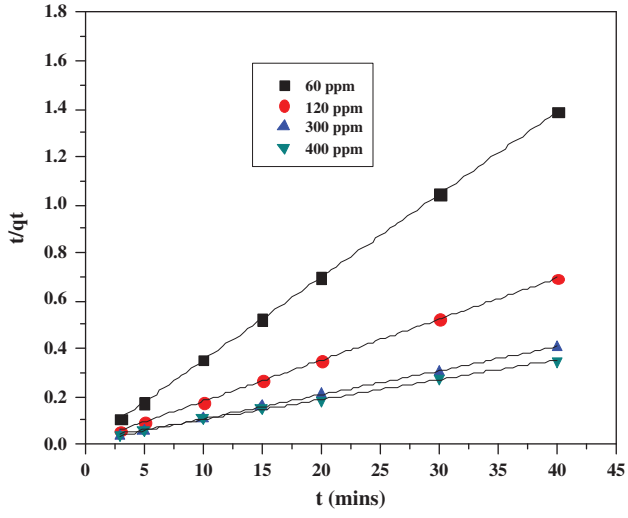

Fig. 9. Pseudo-second-order plots for the adsorption of MG onto SFTS.

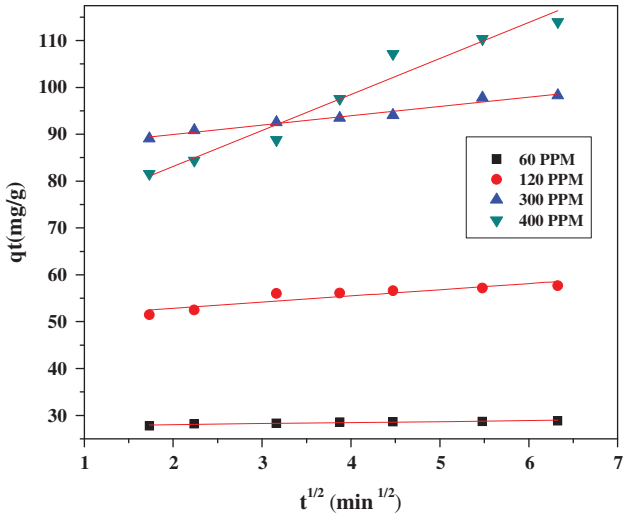

Fig. 10. Intra particle diffusion plots for the adsorption of MG onto SFTS.

where K_{id} is intraparticle diffusion constant (mg/gmin$^{1/2}$) and C_i is the intercept (mg/g). The value of K_{id} and C_i can be obtained from the linear plot of q_t vs. $t^{1/2}$ (Fig. 10) and listed in Table 4. The intraparticle diffusion is the rate-controlling step if the regression of q_t vs. t is linear and passes through the origin. However, linear plots at each concentration did not pass through the origin, confirming intraparticle diffusion is not only the rate-controlling step.

3.7. Desorption studies

Desorption studies can be used to elucidate the mechanism of biosorption process and the possibility of recovery of dye and the biosorbent. Desorption of MG was found to be 1.73% for H_2O, 3.26% for HCl, and 4.1% for CH_3COOH. Very low desorption of MG indicates the formation of some complexes between the active sites of the biosorbent and functional group of the dye molecules. This also suggests that the adsorption of MG onto the surface of SFTS might be chemisorption. The large dye molecules have several contact points with the biosorbent leading to large net adsorption energy, which in turn makes energetically improbable for the dye molecule to be released from the surface of the biosorbent [22,46].

4. Conclusion

Simarouba seed shell was found to be very effective in the removal of MG from aqueous solutions. Langmuir, Freundlich, Temkin, and Dubinin–Radushkevich isotherm models were used to

analyze equilibrium data. The Langmuir adsorption isotherm shows best fit with maximum removal capacity of 125 mg/g. The optimum pH for MG removal was found to be 8. The adsorptive removal of MG follows pseudo-second-order kinetics. The intraparticle diffusion studies reveal that the intraparticle diffusion is not only the rate-limiting step. Desorption studies show the predominant nature of chemisorption of the dye molecules onto the adsorbent surface, which has also been confirmed by the pseudo-second-order kinetics. The studies reveal that Simarouba seed shell can be used as a potential adsorbent for the removal of MG from wastewater.

Acknowledgments

The authors gratefully acknowledge the management of Hindusthan College of Engineering and Technology and Kalaignar Karunanidhi Institute of Technology for providing the instrumentation facilities for the present work.

References

[1] B.H. Hameed, A.A. Ahmad, Batch adsorption of methylene blue from aqueous solution by garlic peel, an agricultural waste biomass, J. Hazard. Mater. 164 (2009) 870–875.
[2] M. Asgher, H.N. Bhatti, Evaluation of thermodynamics and effect of chemical treatments on sorption potential of *Citrus* waste biomass for removal of anionic dyes from aqueous solutions, Ecol. Eng. 38 (2012) 79–85.
[3] B.H. Hameed, M.I. El-Khaiary, Malachite green adsorption by rattan sawdust: Isotherm, kinetic and mechanism modeling, J. Hazard. Mater. 159 (2008) 574–579.
[4] D. Park, Y.-S. Yun, J.M. Park, The past, present, and future trends of biosorption, Biotechnol. Bioprocess Eng. 15 (2010) 86–102.
[5] C. Namasivayam, R.T. Yamuna, Waste biogas residual slurry as an adsorbent for the removal of Pb(II) from aqueous solution and radiator manufacturing industry wastewater, Bioresour. Technol. 52 (1995) 125–131.
[6] N. Gupta, A.K. Kushwaha, M.C. Chattopadhyaya, Adsorption studies of cationic dyes onto Ashoka (*Saraca asoca*) leaf powder, J. Taiwan Inst. Chem. Eng. 43 (2012) 604–613.
[7] G. Zuhra, M.I. Memon, M. Bhanger, F.N. Akhtar, J.R. Talpur, Memon, adsorption of methyl parathion pesticide from water using watermelon peels as a low cost adsorbent, Chem. Eng. J. 138 (2008) 616–621.
[8] M. Doğan, H. Abak, M. Alkan, Adsorption of methylene blue onto hazelnut shell: Kinetics, mechanism and activation parameters, J. Hazard. Mater. 164 (2009) 172–181.
[9] S.D. Khattri, M.K. Singh, Removal of malachite green from dye wastewater using neem sawdust by adsorption, J. Hazard. Mater. 167 (2009) 1089–1094.
[10] B.H. Hameed, Evaluation of papaya seeds as a novel non-conventional low-cost adsorbent for removal of methylene blue, J. Hazard. Mater. 162 (2009) 939–944.
[11] D.K. Venkata Ramana, D. Harikishore Kumar Reddy, J.S. Yu, K. Seshaiah, Pigeon peas hulls waste as potential adsorbent for removal of Pb(II) and Ni(II) from water, Chem. Eng. J. 197 (2012) 24–33.
[12] M.C. Somasekhara Reddy, L. Sivaramakrishna, A. Varada Reddy, The use of an agricultural waste material, Jujuba seeds for the removal of anionic dye (Congo red) from aqueous medium, J. Hazard. Mater. 203–204 (2012) 118–127.
[13] M.T. Yagub, T.K. Sen, M. Ang, Removal of cationic dye methylene blue (MB) from aqueous solution by ground raw and base modified pine cone powder, Environ. Earth Sci. 71 (2014) 1507–1519.
[14] M.S. Sajab, C.H. Chia, S. Zakaria, P.S. Khiew, Cationic and anionic modifications of oil palm empty fruit bunch fibers for the removal of dyes from aqueous solutions, Bioresour. Technol. 128 (2013) 571–577.
[15] A.S. Sartape, A.M. Mandhare, V.V. Jadhav, P.D. Raut, M.A. Anuse, S.S. Kolekar, Removal of malachite green dye from aqueous solution with adsorption technique using *Limonia acidissima* (wood apple) shell as low cost adsorbent, Arab. J. Chem. (2014), doi: 10.1016/j.arabjc.2013.12.019.
[16] A. Nath, S. Chakraborty, C. Bhattacharjee, Bioadsorption of industrial dyes from aqueous solution onto water hyacinth (*Eichornia crassipes*): Equilibrium, kinetic and sorption mechanism study, Desalin. Water Treat. 52 (2014) 1484–1494.
[17] D. Podstawczyk, A. Witek-Krowiak, K. Chojnacka, Z. Sadowski, Biosorption of malachite green by egg shells: Mechanism identification and process optimization, Bioresour. Technol. 160 (2014) 161–165.
[18] A. Witek-Krowiak, Biosorption of malachite green from aqueous solutions by pine sawdust: Equilibrium, kinetics and the effect of process parameters, Desalin. Water Treat. 51 (2013) 3284–3294.
[19] T.S. Anirudhan, P.G. Radhakrishnan, Kinetic and equilibrium modelling of Cadmium(II) ions sorption onto polymerized tamarind fruit shell, Desalination 249 (2009) 1298–1307.
[20] S. Srivastava, R. Sinha, D. Roy, Toxicological effects of malachite green, Aquat. Toxicol. 66 (2004) 319–329.
[21] P.K. Devan, N.V. Mahalakshmi, Utilization of unattended methyl ester of paradise oil as fuel in diesel engine, Fuel 88 (2009) 1828–1833.
[22] M.E. Fernandez, G.V. Nunell, P.R. Bonelli, A.L. Cukierman, Effectiveness of *Cupressus sempervirens* cones as biosorbent for the removal of basic dyes from aqueous solutions in batch and dynamic modes, Bioresour. Technol. 101 (2010) 9500–9507.
[23] K. Anoop, A. Krishnan, Haridas, Removal of phosphate from aqueous solutions and sewage using natural and surface modified coir pith, J. Hazard. Mater. 152 (2008) 527–535.
[24] S. Benyoucef, M. Amrani, Adsorption of phosphate ions onto low cost Aleppo pine adsorbent, Desalination 275 (2011) 231–236.
[25] C. Namasivayam, D. Kavitha, IR, XRD and SEM studies on the mechanism of adsorption of dyes and phenols by coir pith carbon from aqueous phase, Microchem. J. 82 (2006) 43–48.

[26] L. Wang, J. Zhang, R. Zhao, C. Li, Y. Li, C. Zhang, Adsorption of basic dyes on activated carbon prepared from *Polygonum orientale* Linn: Equilibrium, kinetic and thermodynamic studies, Desalination 254 (2010) 68–74.
[27] R.T. Yamuna, C. Namasivayam, Color removal from aqueous solution by biogas residual slurry, Toxicol. Environ. Chem 38(3–4) (1993) 131–143.
[28] R. Gong, Y. Jin, F. Chen, J. Chen, Z. Liu, Enhanced malachite green removal from aqueous solution by citric acid modified rice straw, J. Hazard. Mater. 137 (2006) 865–870.
[29] S. Chowdhury, P. Saha, Sea shell powder as a new adsorbent to remove Basic Green 4 (malachite green) from aqueous solutions: Equilibrium, kinetic and thermodynamic studies, Chem. Eng. J. 164 (2010) 168–177.
[30] M.A. Ahmad, R. Alrozi, Removal of malachite green dye from aqueous solution using rambutan peel-based activated carbon: Equilibrium, kinetic and thermodynamic studies, Chem. Eng. J. 171 (2011) 510–516.
[31] C. Xia, Y. Jing, Y. Jia, D. Yue, J. Ma, X. Yin, Adsorption properties of congo red from aqueous solution on modified hectorite: Kinetic and thermodynamic studies, Desalination 265 (2011) 81–87.
[32] T. Santhi, S. Manonmani, T. Smitha, Removal of malachite green from aqueous solution by activated carbon prepared from the epicarp of *Ricinus communis* by adsorption, J. Hazard. Mater. 179 (2010) 178–186.
[33] C. Namasivayam, R.T. Yamuna, Studies on chromium (III) removal from aqueous solution by adsorption onto biogas residual slurry and its application to tannery wastewater treatment, Water Air Soil Pollut. 113 (1999) 371–384.
[34] B.H. Hameed, M.I. El-Khaiary, Batch removal of malachite green from aqueous solutions by adsorption on oil palm trunk fibre: Equilibrium isotherms and kinetic studies, J. Hazard. Mater. 154 (2008) 237–244.
[35] A. Mittal, Adsorption kinetics of removal of a toxic dye, malachite green, from wastewater by using hen feathers, J. Hazard. Mater. 133 (2006) 196–202.
[36] N. Gupta, A.K. Kushwaha, M.C. Chattopadhyaya, Application of potato (Solanumtuberosum) plant wastes for the removal of methylene blue and malachite green dye from aqueous solution, Arab. J. Chem. (2011), doi: 10.1016/j.arabjc.2011.07.021.
[37] R. Ahmad, R. Kumar, Adsorption studies of hazardous malachite green onto treated ginger waste, J. Environ. Manage. 91 (2010) 1032–1038.
[38] A.A. Jalil, S. Triwahyono, M.R. Yaakob, Z.Z.A. Azmi, N. Sapawe, N.H.N. Kamarudin, H.D. Setiabudi, N.F. Jaafar, S.M. Sidik, S.H. Adam, B.H. Hameed, Utilization of bivalve shell-treated *Zea mays* L. (maize) husk leaf as a low-cost biosorbent for enhanced adsorption of malachite green, Bioresour. Technol. 120 (2012) 218–224.
[39] B.H. Hameed, D.K. Mahmoud, A.L. Ahmad, Equilibrium modeling and kinetic studies on the adsorption of basic dye by a low—Cost adsorbent: Coconut (*Cocos nucifera*) bunch waste, J. Hazard. Mater. 158 (2008) 65–72.
[40] M.A. Khan, M. Ngabura, T.S.Y. Choong, H. Masood, L.A. Chuah, Biosorption and desorption of nickel on oil cake: Batch and column studies, Bioresour. Technol. 103 (2012) 35–42.
[41] H. El Bakouri, J. Usero, J. Morillo, A. Ouassini, Adsorptive features of acid-treated olive stones for drin pesticides: Equilibrium, kinetic and thermodynamic modeling studies, Bioresour. Technol. 100 (2009) 4147–4155.
[42] V.K. Gupta, M.R. Ganjali, A. Nayak, B. Bhushan, S. Agarwal, Enhanced heavy metals removal and recovery by mesoporous adsorbent prepared from waste rubber tire, Chem. Eng. J. 197 (2012) 330–342.
[43] A. Nemr, O. Abdelwahab, A. El-Sikaily, A. Khaled, Removal of direct blue-86 from aqueous solution by new activated carbon developed from orange peel, J. Hazard. Mater. 161 (2009) 102–110.
[44] S. Chen, Q. Yue, B. Gao, Q. Li, X. Xu, Removal of Cr (VI) from aqueous solution using modified corn stalks: Characteristic, equilibrium, kinetic and thermodynamic study, Chem. Eng. J. 168 (2011) 909–917.
[45] A. Witek-Krowiak, Analysis of temperature—Dependent biosorption of Cu^{2+} ions on sunflower hulls: Kinetics, equilibrium and mechanism of the process, Chem. Eng. J. 192 (2012) 13–20.
[46] H.M.H. Gad, A.A. El-Sayed, Activated carbon from agricultural by-products for the removal of Rhodamine-B from aqueous solution, J. Hazard. Mater. 168 (2009) 1070–1081.